Journal of Alloys and Compounds 800 (2019) 247–253

Contents lists available at ScienceDirect

Journal of Alloys and Compounds

journal homepage: http://www.elsevier.com/locate/jalcom

Comparison of anion and cation dynamics in a carbon-substituted *closo*-hydroborate salt: ^{1}H and ^{23}Na NMR studies of solid-solution $Na_2(CB_9H_{10})(CB_{11}H_{12})$

A.V. Soloninin [a], R.V. Skoryunov [a], O.A. Babanova [a], A.V. Skripov [a, *], M. Dimitrievska [b, c], T.J. Udovic [b]

[a] Institute of Metal Physics, Ural Branch of the Russian Academy of Sciences, Ekaterinburg, 620108, Russia
[b] NIST Center for Neutron Research, National Institute of Standards and Technology, Gaithersburg, MD, 20899-6102, USA
[c] National Renewable Energy Laboratory, Golden, CO, 80401, USA

ARTICLE INFO

Article history:
Received 27 March 2019
Received in revised form
24 May 2019
Accepted 3 June 2019
Available online 5 June 2019

Keywords:
Energy storage materials
Diffusion
Nuclear resonances

ABSTRACT

The hexagonal mixed-anion solid solution $Na_2(CB_9H_{10})(CB_{11}H_{12})$ shows the highest room-temperature ionic conductivity among all known Na-ion conductors. To study the dynamical properties of this compound, we have measured the ^{1}H and ^{23}Na nuclear magnetic resonance (NMR) spectra and spin-lattice relaxation rates in $Na_2(CB_9H_{10})(CB_{11}H_{12})$ over the temperature range of 80–435 K. It is found that the diffusive motion of Na^+ ions can be described in terms of two jump processes: the fast localized motion within the pairs of tetrahedral interstitial sites of the hexagonal close-packed lattice formed by large anions and the slower jump process via octahedral sites leading to long-range diffusion. Below 350 K, the slower Na^+ jump process is characterized by the activation energy of 353(11) meV. Although Na^+ mobility in $Na_2(CB_9H_{10})(CB_{11}H_{12})$ found from our NMR experiments is higher than in other ionic conductors, it appears to be an order-of-magnitude lower than that expected on the basis of the conductivity measurements. This result suggests that the complex diffusion mechanism and/or correlations between Na^+ jumps should be taken into account. The measured ^{1}H spin-lattice relaxation rates for $Na_2(CB_9H_{10})(CB_{11}H_{12})$ are consistent with a coexistence of at least two anion reorientational jump processes occurring at different frequency scales. Near room temperature, both reorientational processes are found to be faster than the Na^+ jump process responsible for the long-range diffusion.

1. Introduction

It has been found recently that the disordered phases of a number of *closo*-hydroborate salts, such as $Na_2B_{12}H_{12}$, $Na_2B_{10}H_{10}$, $MCB_{11}H_{12}$, and MCB_9H_{10} (M = Li, Na), exhibit extremely high ionic conductivities [1–4]. These compounds are considered as promising solid electrolytes for Li- and Na-ion batteries [5]. The characteristic feature of these compounds is the occurrence of the order-disorder phase transitions accompanied by abrupt acceleration of both the reorientational (rotational) motion of *closo*-hydroborate anions and the diffusive motion of metal cations [6–10]. Typically, the corresponding jump rates change by 2–3 orders of magnitude near the phase transition points [6,7,9,10]. Since the disordered superionic phases of the *closo*-hydroborate salts are characterized by both high reorientational anion mobility and high diffusive cation mobility, it is reasonable to assume that these two types of motion may be related. Indeed, recent *ab initio* calculations have demonstrated that reorientations of large *closo*-hydroborate anions can facilitate the cation mobility [11–14].

From the experimental point of view, it is important to compare the anion and cation jump rates in the disordered phases of these compounds. In principle, this can be done using nuclear magnetic resonance (NMR) measurements of the spin-lattice relaxation rates for protons (^{1}H) and cation nuclei (^{7}Li, ^{23}Na). However, the cation jump rates have not been measured so far in any *closo*-hydroborate salts because of the absence of the characteristic spin-lattice relaxation rate maximum for cation nuclei [2,4,6,9]. For systems showing atomic jump motion, the spin-lattice relaxation rate maximum is usually observed at the temperature at which the atomic jump rate τ^{-1} becomes nearly equal to the NMR frequency

* Corresponding author.
E-mail address: skripov@imp.uran.ru (A.V. Skripov).

https://doi.org/10.1016/j.jallcom.2019.06.019
0925-8388/

ω [15]. However, due to the abrupt changes in τ^{-1} at the order-disorder phase transitions, the spin-lattice relaxation rate peak for cation nuclei in *closo*-hydroborate salts appears to be "folded", i.e., at the transition point, the relaxation rate jumps from the low-*T* slope of the peak directly to the high-*T* slope [2,4,6,9]. The absence of the relaxation rate maximum does not allow to determine the actual values of τ^{-1} for diffusive motion of cations; only the corresponding activation energies can be derived from the data.

Recently, it has been shown [16–18] that the order-disorder phase transition is suppressed in mixed-anion solid solutions combining nearly spherical (icosahedral) anions, such as $[B_{12}H_{12}]^{2-}$ or $[CB_{11}H_{12}]^{-}$, and ellipsoidal (bicapped-square-antiprismatic) anions, such as $[B_{10}H_{10}]^{2-}$ or $[CB_9H_{10}]^{-}$ (see Fig. 1). These solid solutions retain the disordered state with high ionic conductivity down to low temperatures. Similar behavior has also been found for the mixed-anion solid solution combining the nearly spherical monovalent $[CB_{11}H_{12}]^{-}$ and divalent $[B_{12}H_{12}]^{2-}$ anions, $Na_{2-x}(CB_{11}H_{12})_x(B_{12}H_{12})_{1-x}$ [19]. The suppression of the order-disorder transition gives an opportunity to compare the anion and cation dynamics in the same superionic system. In the present work, we use ^{1}H and ^{23}Na NMR measurements of the spectra and spin-lattice relaxation rates over wide temperature ranges to compare the anion and cation motional parameters in the mixed-anion solid solution $Na_2(CB_9H_{10})(CB_{11}H_{12})$ showing the highest room-temperature ionic conductivity (~0.07 S/cm [17]) among all the studied Na-ion conductors. It should be noted that the results of preliminary ^{1}H spin-lattice relaxation measurements in $Na_2(CB_9H_{10})(CB_{11}H_{12})$ were reported in our previous work [17] at a single resonance frequency and in the limited temperature range. These results were used mainly to illustrate the suppression of an order-disorder transition in mixed-anion solid solution systems. The ^{23}Na spin-lattice relaxation measurements in such systems have not been reported so far.

2. Experimental details

The parent $NaCB_9H_{10}$ and $NaCB_{11}H_{12}$ compounds were obtained from Katchem [20]. The preparation of the solid-solution $Na_2(CB_9H_{10})(CB_{11}H_{12})$ sample by drying the aqueous solution of equimolar amounts of $NaCB_9H_{10}$ and $NaCB_{11}H_{12}$ was analogous to that described in Ref. [17]. According to X-ray diffraction analysis [17], the dominant phase of $Na_2(CB_9H_{10})(CB_{11}H_{12})$ has the hexagonal close-packed structure with the lattice parameters $a = 6.991(1)$ Å and $c = 11.339(2)$ Å. This phase is isomorphous to that found for the pristine superionic $NaCB_9H_{10}$ above ~310 K [4], but has a slightly larger unit cell. The larger cell dimensions for the solid-solution sample are consistent with the substitution of larger $[CB_{11}H_{12}]^{-}$ anions for $[CB_9H_{10}]^{-}$ anions in the $NaCB_9H_{10}$-like hexagonal disordered structure. The presence of a second trace solid-solution phase of $Na_2(CB_9H_{10})(CB_{11}H_{12})$ (<1 mol.%) corresponds to face-centered-cubic anion polymorphic packing. For NMR experiments, the sample was flame-sealed in a quartz tube under vacuum after the additional annealing at 453 K for 6 h.

NMR measurements were performed on a pulse spectrometer with quadrature phase detection at the frequencies $\omega/2\pi = 14$ and 28 MHz (^{1}H) and 23 MHz (^{23}Na). The magnetic field was provided by a 2.1 T iron-core Bruker magnet. A home-built multinuclear continuous-wave NMR magnetometer working in the range 0.32–2.15 T was used for field stabilization. For rf pulse generation, we used a home-built computer-controlled pulse programmer, the PTS frequency synthesizer (Programmed Test Sources, Inc.), and a 1 kW Kalmus wideband pulse amplifier. Typical values of the $\pi/2$ pulse length were 2–3 μs for both nuclei. A probehead with the sample was placed into an Oxford Instruments CF1200 continuous-flow cryostat using nitrogen as a cooling agent. The sample temperature, monitored by a chromel-(Au-Fe) thermocouple, was stable to ±0.1 K. The nuclear spin-lattice relaxation rates were measured using the saturation–recovery method. NMR spectra were recorded by Fourier transforming the solid echo signals (pulse sequence $\pi/2_x - t - \pi/2_y$).

For all figures, standard uncertainties are commensurate with the observed scatter in the data, if not explicitly designated by vertical error bars.

3. Results and discussion

3.1. ^{1}H and ^{23}Na NMR spectra

The evolution of the measured proton NMR spectra with temperature for $Na_2(CB_9H_{10})(CB_{11}H_{12})$ is shown in Fig. 2. It can be seen that both the shape and width of the ^{1}H NMR spectrum are temperature-dependent, and the line width decreases with

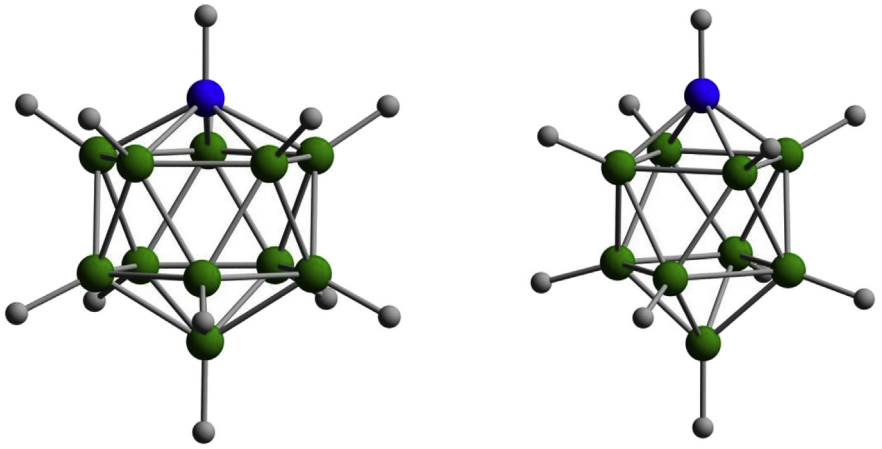

Fig. 1. Schematic view of the nearly spherical (icosahedral) $CB_{11}H_{12}^-$ and ellipsoidal (bicapped-square-antiprismatic) $CB_9H_{10}^-$ anions. Green spheres: B atoms, blue spheres: C atoms, and gray spheres: H atoms. The corresponding C_5 and C_4 symmetry axes are oriented vertically. (For interpretation of the references to colour in this figure legend, the reader is referred to the Web version of this article.)

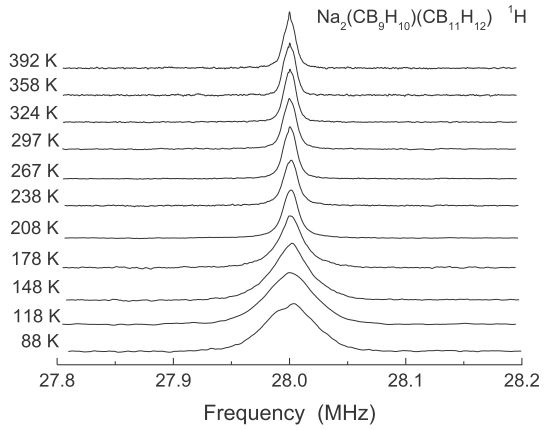

Fig. 2. Evolution of the measured ^{1}H NMR spectra at 28 MHz with temperature for $Na_2(CB_9H_{10})(CB_{11}H_{12})$.

increasing temperature. Such a behavior can be attributed to a partial averaging of the dipole-dipole interactions of ^{1}H spins due to reorientational anion motion. The motional narrowing is expected to be substantial at the temperature at which the H jump rate $\tau_H^{-1}(T)$ becomes comparable to the "rigid lattice" line width Δ_{HR} [15]; for typical complex hydrides, Δ_{HR} is of the order of 10^4–10^5 s^{-1}.

The temperature dependence of the measured ^{1}H line width Δ_H (full width at half-maximum) is shown in Fig. 3. At low temperatures ($T < 110$ K), the line width is nearly constant, and its value ($\Delta_H \approx 49$ kHz) is close to the corresponding low-T values of Δ_H for both $NaCB_9H_{10}$ (~50 kHz [10]) and $NaCB_{11}H_{12}$ (~45 kHz [9]). However, the onset of the motional narrowing for $Na_2(CB_9H_{10})(CB_{11}H_{12})$ occurs at a considerably lower temperature (~120 K) than that for $NaCB_9H_{10}$ (~160 K [10]) and $NaCB_{11}H_{12}$ (~200 K [9]). Hence, the reorientational anion motion in the solid-solution sample at low temperatures appears to be considerably faster than in both pristine $NaCB_9H_{10}$ and $NaCB_{11}H_{12}$ salts; this is consistent with the fact that the solid-solution sample retains the disordered state down to low temperatures. At $T > 300$ K, the proton NMR line width for $Na_2(CB_9H_{10})(CB_{11}H_{12})$ reaches a plateau, being close to 12 kHz. Such a plateau region is typical of reorientational motion of H-containing groups [21]. In contrast to long-range translational diffusion that leads to complete averaging of the dipole-dipole interactions of ^{1}H spins, the averaging due to localized (reorientational) motion is only partial, even in the case when $\tau_H^{-1} \gg 2\pi\Delta_{HR}$. It is usually assumed that, for the plateau region, the dipole-dipole interactions within the reorienting groups ("intramolecular" interactions) are completely averaged out, while the interactions between ^{1}H spins on different groups ("intermolecular" interactions) are not averaged.

Fig. 4 shows the evolution of the ^{23}Na NMR spectra for $Na_2(CB_9H_{10})(CB_{11}H_{12})$ in the temperature range 98–435 K. As can be seen from this figure, the ^{23}Na NMR spectrum exhibits strong narrowing with increasing temperature. General features of the ^{23}Na line shape behavior are typical of those observed for Na-ion conductors (see, for example, recent results for NASICON-type compound $Na_{3.4}Sc_2(SiO_4)_{0.4}(PO_4)_{2.6}$ [22]). It should be noted that the high-temperature ^{23}Na NMR line width Δ_{Na} (full width at half-maximum) in $Na_2(CB_9H_{10})(CB_{11}H_{12})$ is much smaller than the high-temperature ^{1}H NMR line width Δ_H. Indeed, the observed value of Δ_{Na} at $T > 300$ K is ~0.7 kHz, whereas the value of Δ_H in the same temperature range is about 12 kHz. This indicates that, in contrast to the case of H motion, Na ions participate in the *long-range* diffusion which is expected to average out both the dipole-dipole interactions and the electric quadrupole interactions of ^{23}Na nuclei.

The temperature dependence of the measured ^{23}Na line width is shown in Fig. 5. As can be seen from this figure, $\Delta_{Na}(T)$ exhibits two pronounced motional narrowing "steps" near 180 K and near 250 K. Such a behavior suggests a presence of two motional processes responsible for the line narrowing. It is evident that the main (high-temperature) "step" corresponds to the excitation of the long-range Na^+ diffusion at the frequency scale of about 10^4 s^{-1}. The line width "step" near 180 K requires an additional consideration. Can this minor "step" originate from reorientational anion motion modulating the ^{23}Na – ^{1}H dipole-dipole interaction? While this mechanism seems to be probable, a comparison of the $\Delta_{Na}(T)$ data (Fig. 5) with the behavior of $\Delta_H(T)$ (Fig. 3) indicates that the main changes in the proton line width occur at considerably lower temperatures than the minor "step" of the ^{23}Na line width. It is likely that the reorientational anion motion is responsible just for the gradual decrease in Δ_{Na} in the temperature range 100–180 K (Fig. 5). It should also be noted that anion reorientations are not expected to affect the electric field gradients (EFG) at ^{23}Na sites, since each reorientational jump does not change the charge configuration around these sites. However, if Na^+ cations themselves start to move, we may expect stronger effects on the ^{23}Na line width.

In order to discuss a possible origin of two frequency scales of Na^+ jump motion, we have to consider the sublattice of partially-filled Na sites in $Na_2(CB_9H_{10})(CB_{11}H_{12})$. According to the structural results [17], this sublattice is represented by tetrahedral (T)

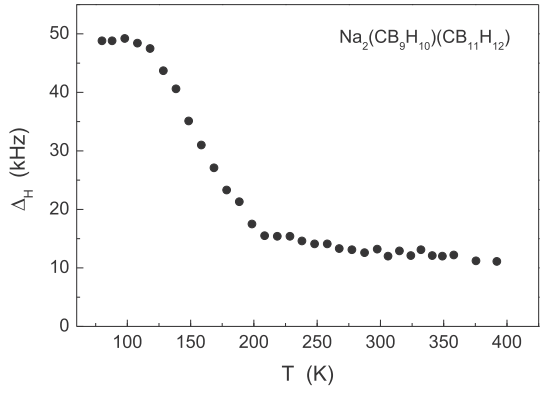

Fig. 3. Temperature dependence of the width (full width at half-maximum) of the ^{1}H NMR spectrum measured for $Na_2(CB_9H_{10})(CB_{11}H_{12})$ at 28 MHz.

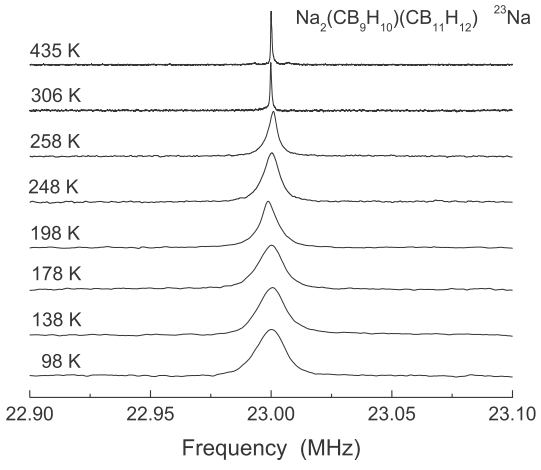

Fig. 4. Evolution of the measured ^{23}Na NMR spectra with temperature for $Na_2(CB_9H_{10})(CB_{11}H_{12})$.

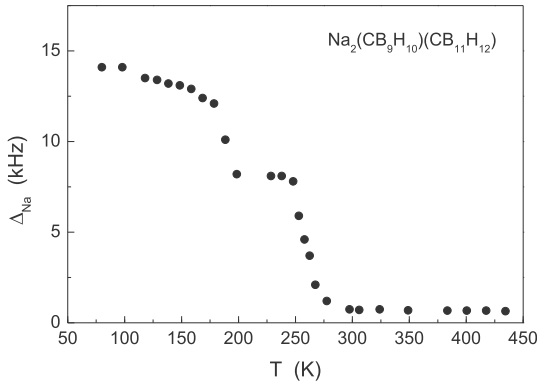

Fig. 5. Temperature dependence of the width (full width at half-maximum) of the ^{23}Na NMR line for $Na_2(CB_9H_{10})(CB_{11}H_{12})$.

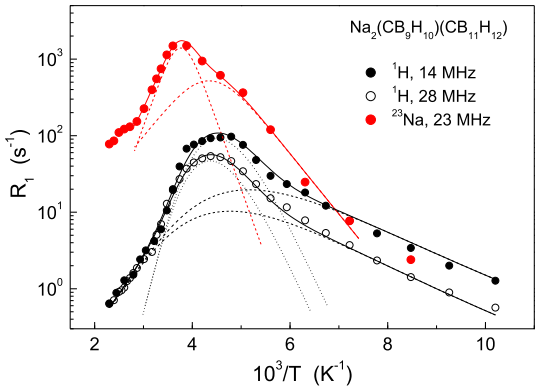

Fig. 7. Proton spin-lattice relaxation rates measured at 14 and 28 MHz and ^{23}Na spin-lattice relaxation rates measured at 23 MHz as functions of the inverse temperature. Black solid lines show the simultaneous fit of the two-peak model with Gaussian distributions of the activation energies to the $R_1^H(T)$ data in the range 98–435 K; the black dashed and dotted lines represent the contributions of the two components. The red solid line shows the fit of the two-peak model to the $R_1^{Na}(T)$ data in the range 138–349 K; the red dashed lines represent the contributions of the two components. (For interpretation of the references to colour in this figure legend, the reader is referred to the Web version of this article.)

and octahedral (O) interstitial sites of the hexagonal close-packed lattice, see Fig. 6. The interesting feature of this sublattice is the existence of closely-spaced pairs of T-sites along the *c* axis. The distance between T-sites within such a pair (~2.84 Å) is considerably smaller than the distances between the nearest-neighbor T and O sites (~4.28 Å) or between T sites belonging to different pairs (~4.93 Å). Therefore, back-and-forth Na^+ jumps within the T-T pairs (not contributing to long-range diffusion) are expected to have higher rates than the T-O jumps (leading to long-range diffusion). It is reasonable to assume that such a localized Na^+ motion within the T-T pairs is responsible for the minor $\Delta_{Na}(T)$ "step" near 180 K. Similar localized motion was previously reported for H atoms occupying the tetrahedral interstitial sites in hcp scandium [23–25] and in bcc niobium doped with oxygen [26].

3.2. ^{1}H and ^{23}Na spin-lattice relaxation rates

Fig. 7 shows the behavior of the proton spin-lattice relaxation rate R_1^H (measured at two resonance frequencies $\omega/2\pi$) and the ^{23}Na spin-lattice relaxation rate R_1^{Na} as functions of the inverse temperature. It can be seen that both $R_1^H(T)$ and $R_1^{Na}(T)$ exhibit peaks; however, these peaks are shifted with respect to each other. As discussed in the Introduction, a nuclear spin-lattice relaxation rate maximum is expected to occur at the temperature at which the corresponding atomic jump rate becomes nearly equal to the resonance frequency. We shall start with a discussion of the proton spin-lattice relaxation which is governed by ^{1}H–^{1}H and ^{1}H–^{11}B dipole-dipole interactions modulated by anion reorientations. According to the standard theory of nuclear spin-lattice relaxation due to the motionally modulated dipole-dipole interaction [15,27], in the limit of slow motion ($\omega\tau_H \gg 1$), R_1^H should be proportional to $\omega^{-2}\tau_H^{-1}$, and in the limit of fast motion ($\omega\tau_H \ll 1$), R_1^H should be proportional to τ_H, being frequency-independent. If the temperature dependence of the H jump rate τ_H^{-1} follows the Arrhenius law,

$$\tau_H^{-1} = \tau_{H0}^{-1} \exp(-E_a/k_BT) \quad (1)$$

with the activation energy E_a for the reorientational motion, the plot of $\ln R_1^H$ versus T^{-1} is expected to be linear in the limits of both slow and fast motion with the slopes of $-E_a/k_B$ and E_a/k_B, respectively. As can be seen from Fig. 7, the experimental $R_1^H(T)$ data for $Na_2(CB_9H_{10})(CB_{11}H_{12})$ show strong deviations from the predictions of the standard model. In particular, there are changes in the slopes of the $\ln R_1^H$ vs. T^{-1} plot both above and below the relaxation rate maximum. Furthermore, the observed frequency dependence of R_1^H at the low-temperature slope of the relaxation rate peak is considerably weaker than the predicted ω^{-2} dependence. These features suggest a coexistence of at least two reorientational processes with different characteristic jump rates τ_{Hi}^{-1} ($i = 1, 2$) and with a distribution of jump rates [28] for each of the processes. For our disordered mixed-anion solid solution, such a behavior may be expected, since each anion can participate in different types of reorientations [10]; furthermore, there are two types of anions, and their local environments vary from one anion to the next. It should be noted that the use of a certain distribution of jump rates is necessary to describe [28] the reduced frequency dependence of R_1^H mentioned above. Thus, for parametrization of the $R_1^H(T)$ data, we have used the simplest two-peak model assuming a coexistence of two jump processes, each of which is characterized by a Gaussian distribution of the activation energies. For this model, the observed

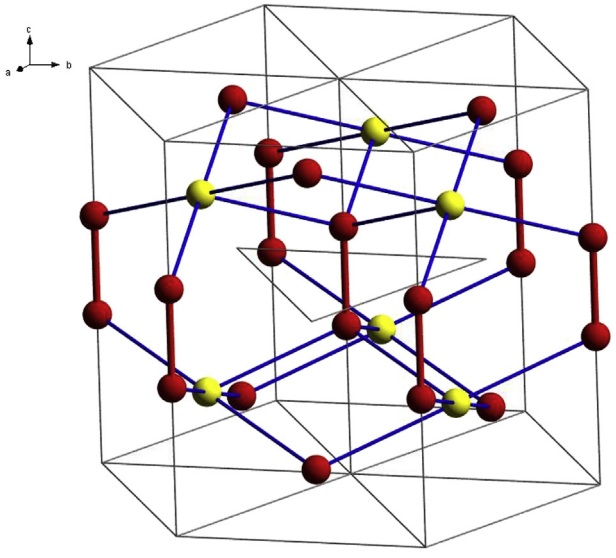

Fig. 6. The sublattice of partially-filled Na sites and possible Na^+ diffusion paths within the hexagonal close-packed elementary cell of $Na_2(CB_9H_{10})(CB_{11}H_{12})$. Red spheres: tetrahedral (T) sites, and yellow spheres: octahedral (O) sites. Red bars connect the closely-spaced pairs of T sites, and dark blue bars connect the nearest-neighbor T and O sites. (For interpretation of the references to colour in this figure legend, the reader is referred to the Web version of this article.)

proton spin-lattice relaxation rate is expressed as

$$R_1^H = \sum_{i=1}^{2} R_{1i}^H, \quad (2)$$

$$R_{1i}^H = \int R_{1i}^H(E_{ai}) G(E_{ai}, \overline{E}_{ai}, \Delta E_{ai}) dE_{ai} \quad (3)$$

Here $G(E_{ai}, \overline{E}_{ai}, \Delta E_{ai})$ is a Gaussian distribution function centered on $\overline{E}_{ai}$ with the dispersion ΔE_{ai}, $G(E_{ai}, \overline{E}_{ai}, \Delta E_{ai}) = (1/\sqrt{2\pi}\,\Delta E_{ai})\exp[-(E_{ai} - \overline{E}_{ai})^2/2(\Delta E_{ai})^2]$, and $R_{1i}^H(E_{ai})$ is determined by combining the standard expression that relates the spin-lattice relaxation rate with τ_{Hi}^{-1} (see Supplementary Information) and the Arrhenius law (Equation (1)) for the ith process. The parameters of the model are the average activation energies $\overline{E}_{ai}$, the dispersions ΔE_{ai}, the pre-exponential factors τ_{H0i} of the Arrhenius law, and the amplitude factors ΔM_i determined by the strength of the fluctuating parts of dipole-dipole interactions for each of the jump processes. These parameters have been varied to find the best fit to the $R_1^H(T)$ data at two resonance frequencies *simultaneously*. The results of the simultaneous fit over the T range of 98–435 K are shown by black solid lines in Fig. 7; the corresponding parameters are $\overline{E}_{a1} = 147(9)$ meV, $\Delta E_{a1} = 31(5)$ meV, $\tau_{H01} = 1.2(2) \times 10^{-12}$ s, and $\Delta M_1 = 1.0(2) \times 10^9$ s^{-2} for the faster jump process, and $\overline{E}_{a2} = 430(40)$ meV, $\Delta E_{a2} = 41(8)$ meV, $\tau_{H02} = 1.6(3) \times 10^{-18}$ s, and $\Delta M_2 = 5.2(2) \times 10^9$ s^{-2} for the slower process. It should be noted that the value of the pre-exponential factor τ_{H02} for the slower process appears to be too small to allow any straightforward physical interpretation. Such a result may be related to the limited temperature range, where the slower process gives the dominant contribution to the observed relaxation rate. The nature of the two reorientational processes cannot be determined unambiguously from the available experimental data. The most probable main reason for the two-peak behavior is related to a coexistence of two types of reorientations: the faster jumps of the anions around the C_4 axis for $[CB_9H_{10}]^-$ or the C_5 axis for $[CB_{11}H_{12}]^-$ (see Fig. 1) and the slower 180° flips perpendicular to the C_4 or C_5 axis. These two types of reorientations are consistent with quasielastic neutron scattering (QENS) results for the disordered phase of hexagonal $NaCB_9H_{10}$ [10]. It is interesting to compare the average activation energy $\overline{E}_{a1}$ that determines the high-temperature behavior of $R_1^H(T)$ for $Na_2(CB_9H_{10})(CB_{11}H_{12})$ with the corresponding activation energies for the disordered phases of pristine $NaCB_9H_{10}$ and $NaCB_{11}H_{12}$. The value of $\overline{E}_{a1}$ found in the present work (147(9) meV) appears to be somewhat lower than the high-T activation energies derived from NMR experiments (205 meV for $NaCB_9H_{10}$ [10] and 177 meV for $NaCB_{11}H_{12}$ [9]), but somewhat higher than those derived from QENS experiments (130 meV for $NaCB_9H_{10}$ [10] and 114 meV for $NaCB_{11}H_{12}$ [14]).

As noted above, because of the order-disorder phase transitions, a regular ^{23}Na spin-lattice relaxation rate maximum has not been observed for the pristine compounds $Na_2B_{12}H_{12}$ [6], $Na_2B_{10}H_{10}$ [10], $NaCB_{11}H_{12}$ [9], and $NaCB_9H_{10}$ [10]. The appearance of the $R_1^{Na}(T)$ maximum for the mixed-anion solid solution $Na_2(CB_9H_{10})(CB_{11}H_{12})$ (Fig. 7) allows us to make certain conclusions concerning the diffusive Na^+ jump rate τ_{Na}^{-1} and the interactions responsible for the $R_1^{Na}(T)$ peak. First, it should be noted that the amplitude of the $R_1^{Na}(T)$ peak is much higher than that of the $R_1^H(T)$ peak at comparable resonance frequencies (see Fig. 7). This feature suggests that the observed ^{23}Na spin-lattice relaxation rate is dominated by the quadrupole mechanism related to EFG fluctuations at ^{23}Na sites, since the dipole-dipole interactions between nuclear spins are too weak to give rise to such fast relaxation. However, anion reorientations cannot be responsible for the dominant quadrupole relaxation mechanism, since each reorientational jump does not change the charge configuration around ^{23}Na sites. This is also supported by the fact that the observed temperature dependence of R_1^{Na} strongly differs from that of R_1^H (see Fig. 7). On the other hand, any jump of Na^+ from one site of the cation sublattice to another is expected to change the principal EFG value and/or the angle between the principal axis of the EFG tensor and the magnetic field direction, providing the effective quadrupole relaxation mechanism. It should also be noted that, in some systems, the characteristic rate of EFG fluctuations differs from the jump rate of diffusive atomic motion [29,30]. This may occur in the case when the local symmetry of sites occupied by diffusing ions is cubic, so that EFG fluctuations originate solely from transient occupation of some of the neighboring interstitial sites by other diffusing ions, which leads to non-negligible effects of three-particle correlations [29,30]. However, in our solid-solution system, the local symmetry of Na^+ sites is lower than cubic, and we can expect that the characteristic rate of EFG fluctuations is equal to the Na^+ jump rate.

The simplest approach to describe the motionally induced quadrupole contribution to the spin-lattice relaxation rate is based on the expression

$$R_1^{Na} = \frac{M_Q}{\omega}\left[\frac{y}{1+y^2} + \frac{4y}{1+4y^2}\right], \quad (4)$$

where $y = \omega\tau_{Na}$. Here the amplitude factor M_Q is proportional to the square of the electric quadrupole moment of ^{23}Na and the mean square of the fluctuating part of EFG at ^{23}Na sites due to diffusive jumps. It should be noted that the basic features of the dependence of this quadrupole contribution on ω and τ are similar to those of the motionally induced dipole-dipole contribution. In particular, the $R_1^{Na}(T)$ maximum should occur at the temperature at which the diffusive jump rate τ_{Na}^{-1} becomes nearly equal to ω. Since the $R_1^{Na}(T)$ maximum is observed at the higher temperature than the $R_1^H(T)$ maximum (see Fig. 7), we can conclude that the cation jump rate τ_{Na}^{-1} is considerably lower than the anion reorientational rate, at least in the region of the peaks. A closer inspection of the $R_1^{Na}(T)$ peak in Fig. 7 reveals the presence of an inflection point at the low-T slope of this peak; this suggests a coexistence of two jump processes for Na^+ ions, in agreement with the ^{23}Na NMR line width results discussed above.

Therefore, for parametrization of the $R_1^{Na}(T)$ data in the range 138–349 K we have used the two-peak model assuming a coexistence of two Na^+ jump processes with the rates τ_{Naj}^{-1} ($j = 1, 2$); each of the rates is governed by its own Arrhenius law with individual pre-exponential factors and the activation energies E_{aj}^d for diffusive jumps. It should be noted that, according to the discussion of possible diffusive jumps over the cation sublattice (Fig. 6), only the slower of the two Na^+ jump processes (giving rise to the main $R_1^{Na}(T)$ maximum) is responsible for the *long-range* Na^+ diffusion. The red solid line in Fig. 7 shows the fit of this two-peak model to the experimental $R_1^{Na}(T)$ data over the range of 138–349 K; the corresponding parameters are $E_{a1}^d = 156$ (5) meV, $\tau_{Na01} = 1.6$ (1) $\times 10^{-12}$ s, and $M_{Q1} = 5.3$ (1) $\times 10^{10}$ s^{-2} for the faster (localized) jump process, and $E_{a2}^d = 353$ (11) meV, $\tau_{Na02} = 8.8$ (3) $\times 10^{-16}$ s, and $M_{Q2} = 1.4$ (1) $\times 10^{11}$ s^{-2} for the slower jump process related to long-range diffusion. It is interesting to note that the value of E_{a2}^d found from the fit is very close to the activation energy derived from the conductivity measurements for $Na_2(CB_9H_{10})(CB_{11}H_{12})$ at $T < 300$ K (348(2) meV [17]). Neglecting any correlations for diffusive jumps, the tracer diffusion coefficient of Na^+ ions can be estimated as $D = L^2\tau_{Na2}^{-1}/6$, where L is the jump length. The value of the diffusive jump rate estimated at the temperature of the $R_1^{Na}(T)$ maximum is τ_{Na2}^{-1} (263 K) $\approx 2.0 \times 10^8$ s^{-1}. Using the distance of 4.28 Å between the nearest-neighbor T and O sites as the jump

length, we obtain $D(263\,K) \approx 6.1 \times 10^{-8}\,cm^2/s$. This value appears to be rather high; for example, for the NASICON-type Na-ion conductor $Na_{3.4}Sc_2(SiO_4)_{0.4}(PO_4)_{2.6}$, a comparable value of D is reached only at 350 K [22]. The value of the tracer diffusion coefficient can be used to estimate the ionic conductivity σ from the Nernst-Einstein equation

$$\sigma = \frac{nD(Ze)^2}{k_B T}, \quad (5)$$

where n is the number of charge carriers per unit volume and Ze is the electrical charge of the carrier. Using the lattice parameters of $Na_2(CB_9H_{10})(CB_{11}H_{12})$ [17], we find that $n = 4.17 \times 10^{21}\,cm^{-3}$ and $\sigma(263\,K) = 1.8 \times 10^{-3}$ S/cm. The measured ionic conductivity of $Na_2(CB_9H_{10})(CB_{11}H_{12})$ near 263 K (~1.5×10^{-2} S/cm [17]) is an order of magnitude higher than this estimate. It should be noted that according to the complex impedance plots [17], $Na_2(CB_9H_{10})(CB_{11}H_{12})$ represents a purely Na-ion conductor. Therefore, we can conclude that our simple approach underestimates the Na^+ diffusivity. Since D is proportional to L^2, one of the probable reasons is the underestimation of L. This may be related to the complex nature of Na^+ diffusive motion in $Na_2(CB_9H_{10})(CB_{11}H_{12})$, where the fast localized jumps within closely-spaced T sites coexist with the slower jumps between T and O sites. Similar effects were found for hydrogen diffusion in Laves-phase hydrides, where the diffusion path includes fast localized H jumps within the hexagons formed by tetrahedral interstitial sites and slower H jumps from one such hexagon to another [31–33]. In the case of H diffusion in Laves-phase hydrides, it was well-documented that, at the timescale of the slower process responsible for the long-range diffusion, the effective jump length is considerably longer than the distance between the nearest-neighbor sites at the adjacent hexagons [31–33]. Another possible reason for the underestimation of D may be related to correlations between jumps of different cations adjoining a large anion. Indeed, according to the results of recent *ab initio* calculations for $Li_2B_{12}H_{12}$ and $Na_2B_{12}H_{12}$ [13], and for $LiCB_{11}H_{12}$ and $NaCB_{11}H_{12}$ [14], Li^+ and Na^+ cations surrounding a single $B_{12}H_{12}^{2-}$ or $CB_{11}H_{12}^-$ anion have some energetically preferable angular configurations; therefore, a rotation of the anion is expected to facilitate jumps of several cations. Similar mechanisms implying a relation between anion rotation and cation mobility were previously discussed for several other classes of superionic conductors [34–36].

Returning to Fig. 7, we can see the pronounced change in the slope of the log R_1^{Na} vs. T^{-1} plot above 350 K. This change in the slope is not described by the model used above for the fit of the $R_1^{Na}(T)$ data. Such a behavior suggests a change in the activation energy for Na^+ diffusion at high temperatures. It may be related to some changes in the diffusion mechanism leading to the decrease of energy barriers for Na^+ jumps. It should be noted that a similar change in the activation energy was also reported for the ionic conductivity of $Na_2(CB_9H_{10})(CB_{11}H_{12})$ [17], although at somewhat lower temperatures. The value of the activation energy for Na^+ jumps estimated from the slope of the $R_1^{Na}(T)$ data above 350 K is 135(8) meV.

In order to explicitly compare the rates of diffusive Na^+ jumps and anion reorientational jumps in $Na_2(CB_9H_{10})(CB_{11}H_{12})$, we have to choose a certain reference temperature. Since the jump rates are most reliably probed near the corresponding spin-lattice relaxation rate maxima, it is reasonable to choose the reference temperature close to these maxima. Using the fits to the $R_1^{Na}(T)$ and $R_1^{H}(T)$ data, at $T = 273$ K (i. e., close to the temperature of the $R_1^{Na}(T)$ maximum) we obtain: $\tau_{Na2}^{-1}(273\,K) = 3.5 \times 10^8\ s^{-1}$, and the average anion jump rates are $\tau_{H1}^{-1}(273\,K) = 1.6 \times 10^9\ s^{-1}$ and $\tau_{H2}^{-1}(273\,K) = 6.9 \times 10^9\ s^{-1}$. These latter H jump rates are fully consistent with those that can be deduced from previous elastic-neutron-scattering fixed-window scans for $Na_2(CB_9H_{10})(CB_{11}H_{12})$ [17]. The present results show that at the reference temperature the rates of anion reorientational jumps are higher than the rate of cation diffusive jumps. However, the difference between the corresponding frequency scales is not too large, and the results are generally consistent with the notion [13,14] that anion dynamics can contribute to the smoothening of the energy landscape for cation jumps.

4. Conclusions

The analysis of the temperature dependences of the ^{23}Na NMR spectra and spin-lattice relaxation rates in the mixed-anion solid solution $Na_2(CB_9H_{10})(CB_{11}H_{12})$ has shown that the diffusive motion of Na^+ ions in this system can be described in terms of two jump processes: the fast localized motion within the pairs of tetrahedral interstitial sites of the hexagonal close-packed lattice formed by large anions and the slower jump process via octahedral sites leading to long-range diffusion. Below 350 K, the slower Na^+ jump process is characterized by the activation energy of 353(11) meV, and the corresponding jump rate reaches ~ $3 \times 10^8\ s^{-1}$ near 273 K. These results are generally consistent with the exceptional room-temperature ionic conductivity in $Na_2(CB_9H_{10})(CB_{11}H_{12})$, although quantitative agreement between the Na^+ mobility and conductivity data would require a consideration of the complex diffusion mechanism and/or correlations between Na^+ jumps.

The results of the proton spin-lattice relaxation measurements for $Na_2(CB_9H_{10})(CB_{11}H_{12})$ are consistent with a coexistence of at least two anion reorientational jump processes occurring at different frequency scales. Both reorientational processes are found to be faster than the Na^+ jump process responsible for the long-range diffusion. In particular, the corresponding rates reach ~$2 \times 10^9\ s^{-1}$ and ~$7 \times 10^9\ s^{-1}$ near 273 K. These results support the conclusions [13,14] that anion dynamics can contribute to reducing the energy barriers for cation jumps.

Acknowledgments

This work was performed within the assignment of the Russian federal scientific program “Function” No. AAAA-A19-119012990095-0, supported in part by the Russian Foundation for Basic Research (Grant No. 19-03-00133). M.D. gratefully acknowledges support from the US DOE Office of Energy Efficiency and Renewable Energy, Fuel Cell Technologies Office, under Contract No. DE-AC36-08GO28308.

Appendix A. Supplementary data

Supplementary information to this article includes expressions used for analysis of the proton spin-lattice relaxation rates. This information can be found online at https://doi.org/10.1016/j.jallcom.2019.06.019.

References

[1] T.J. Udovic, M. Matsuo, A. Unemoto, N. Verdal, V. Stavila, A.V. Skripov, J.J. Rush, H. Takamura, S. Orimo, Sodium superionic conduction in $Na_2B_{12}H_{12}$, Chem. Commun. 50 (2014) 3750–3752.
[2] T.J. Udovic, M. Matsuo, W.S. Tang, H. Wu, V. Stavila, A.V. Soloninin, R.V. Skoryunov, O.A. Babanova, A.V. Skripov, J.J. Rush, A. Unemoto, H. Takamura, S. Orimo, Exceptional superionic conductivity in disordered sodium decahydro-*closo*-decaborate, Adv. Mater. 26 (2014) 7622–7626.
[3] W.S. Tang, A. Unemoto, W. Zhou, V. Stavila, M. Matsuo, H. Wu, S. Orimo, T.J. Udovic, Unparalleled lithium and sodium superionic conduction in solid electrolytes with large monovalent cage-like anions, Energy Environ. Sci. 8 (2015) 3637–3645.

[4] W.S. Tang, M. Matsuo, H. Wu, V. Stavila, W. Zhou, A.A. Talin, A.V. Soloninin, R.V. Skoryunov, O.A. Babanova, A.V. Skripov, A. Unemoto, S. Orimo, T.J. Udovic, Liquid-like ionic conduction in solid lithium and sodium monocarba-*closo*-decaborates near or at room temperature, Adv. Energy Mater. 6 (2016) 1502237.
[5] K. Yoshida, T. Sato, A. Unemoto, M. Matsuo, T. Ikeshoji, T.J. Udovic, S. Orimo, Fast sodium ionic conduction in $Na_2B_{10}H_{10}$-$Na_2B_{12}H_{12}$ complex hydride and application to a bulk-type all-solid-state battery, Appl. Phys. Lett. 110 (2017) 103901.
[6] A.V. Skripov, O.A. Babanova, A.V. Soloninin, V. Stavila, N. Verdal, T.J. Udovic, J.J. Rush, Nuclear magnetic resonance study of atomic motion in $A_2B_{12}H_{12}$ (A = Na, K, Rb, Cs): anion reorientations and Na^+ mobility, J. Phys. Chem. C 117 (2013) 25961–25968.
[7] N. Verdal, J.-H. Her, V. Stavila, A.V. Soloninin, O.A. Babanova, A.V. Skripov, T.J. Udovic, J.J. Rush, Complex high-temperature phase transitions in $Li_2B_{12}H_{12}$ and $Na_2B_{12}H_{12}$, J. Solid State Chem. 212 (2014) 81–90.
[8] N. Verdal, T.J. Udovic, V. Stavila, W.S. Tang, J.J. Rush, A.V. Skripov, Anion reorientations in the superionic conducting phase of $Na_2B_{12}H_{12}$, J. Phys. Chem. C 118 (2014) 17483–17489.
[9] A.V. Skripov, R.V. Skoryunov, A.V. Soloninin, O.A. Babanova, W.S. Tang, V. Stavila, T.J. Udovic, Anion reorientations and cation diffusion in $LiCB_{11}H_{12}$ and $NaCB_{11}H_{12}$: ^1H, ^7Li, and ^{23}Na NMR studies, J. Phys. Chem. C 119 (2015) 26912–26918.
[10] A.V. Soloninin, M. Dimitrievska, R.V. Skoryunov, O.A. Babanova, A.V. Skripov, W.S. Tang, V. Stavila, T.J. Udovic, Comparison of anion reorientational dynamics in MCB_9H_{10} and $M_2B_{10}H_{10}$ (M = Li, Na) via nuclear magnetic resonance and quasielastic neutron scattering studies, J. Phys. Chem. C 121 (2017) 1000–1012.
[11] Z. Lu, F. Ciucci, Structural origin of the superionic Na conduction in $Na_2B_{10}H_{10}$ *closo*-borates and enhanced conductivity by Na deficiency for high performance solid electrolyte, J. Mater. Chem. 4 (2016) 17740–17748.
[12] J.B. Varley, K. Kweon, P. Mehta, P. Shea, T.W. Heo, T.J. Udovic, V. Stavila, B.C. Wood, Understanding ionic conductivity trends in polyborane solid electrolytes from *ab initio* molecular dynamics, ACS Energy Lett 2 (2017) 250–255.
[13] K. Kweon, J.B. Varley, P. Shea, N. Adelstein, P. Mehta, T.W. Heo, T.J. Udovic, V. Stavila, B.C. Wood, Structural, chemical, and dynamical frustration: origins of superionic conductivity in *closo*-borate solid electrolytes, Chem. Mater. 29 (2017) 9142–9153.
[14] M. Dimitrievska, P. Shea, K.E. Kweon, M. Bercx, J.B. Varley, W.S. Tang, A.V. Skripov, V. Stavila, T.J. Udovic, B.C. Wood, Carbon incorporation and anion dynamics as synergistic drivers for ultrafast diffusion in superionic $LiCB_{11}H_{12}$ and $NaCB_{11}H_{12}$, Adv. Energy Mater. 6 (2018) 1703422.
[15] A. Abragam, The Principles of Nuclear Magnetism, Clarendon Press, Oxford, 1961.
[16] W.S. Tang, M. Matsuo, H. Wu, V. Stavila, A. Unemoto, S. Orimo, T.J. Udovic, Stabilizing lithium and sodium fast-ion conduction in solid polyhedral-borate salts at device-relevant temperatures, Energy Storage Mater 4 (2016) 79–83.
[17] W.S. Tang, K. Yoshida, A.V. Soloninin, R.V. Skoryunov, O.A. Babanova, A.V. Skripov, M. Dimitrievska, V. Stavila, S. Orimo, T.J. Udovic, Stabilizing superionic-conducting structures via mixed-anion solid solutions of monocarba-*closo*-borate salts, ACS Energy Lett 1 (2016) 659–664.
[18] L. Duchêne, R.-S. Kühnel, D. Rentsch, A. Remhof, H. Hagemann, C. Battaglia, A highly stable sodium solid-state electrolyte based on a dodeca/deca-borate equimolar mixture, Chem. Commun. 53 (2017) 4195–4198.
[19] M. Brighi, F. Murgia, Z. Łodziana, P. Schouwink, A. Wołczyk, R. Černý, A mixed anion hydroborate/carba-hydroborate as a room temperature Na-ion solid electrolyte, J. Power Sources 404 (2018) 7–12.
[20] The Mention of All Commercial Suppliers in This Paper Is for Clarity and Does Not Imply the Recommendation or Endorsement of These Suppliers by NIST.
[21] A.V. Skripov, A.,V. Soloninin, O.A. Babanova, R.V. Skoryunov, Nuclear magnetic resonance studies of atomic motion in borohydride-based materials: fast anion reorientations and cation diffusion, J. Alloy. Comp. 645 (2015) S428–S433.
[22] M. Kaus, M. Guin, M. Yavuz, M. Knapp, F. Tietz, O. Guillon, H. Ehrenberg, S. Indris, Fast Na^+ ion conduction in NASICON-type $Na_{3.4}Sc_2(SiO_4)_{0.4}(PO_4)_{2.6}$ observed by ^{23}Na NMR relaxometry, J. Phys. Chem. C 121 (2017) 1449–1454.
[23] L.R. Lichty, J.W. Han, R. Ibanez-Meier, D.R. Torgeson, R.G. Barnes, E.F.W. Seymour, C.A. Sholl, Low-temperature localized motion of hydrogen and electronic structure transition in hexagonal-close-packed scandium, Phys. Rev. B 39 (1989) 2012–2021.
[24] I.S. Anderson, N.F. Berk, J.J. Rush, T.J. Udovic, R.G. Barnes, A. Magerl, D. Richter, Rapid low-temperature hopping of hydrogen in a pure metal: the ScH_x system, Phys. Rev. Lett. 65 (1990) 1439–1442.
[25] J.J. Balbach, M.S. Conradi, R.G. Barnes, D.S. Sibirtsev, A.V. Skripov, Nuclear magnetic resonance study of the low-temperature localized H(D) motion in α-$ScH_x(D_x)$: isotope effects, Phys. Rev. B 60 (1999) 966–971.
[26] T. Pfiz, R. Messer, A. Seeger, Nuclear magnetic resonance (NMR) studies of hydrogen tunneling and trapping in niobium, Z. Phys. Chem. N. F. 164 (1989) 969–974.
[27] N. Bloembergen, E.M. Purcell, R.V. Pound, Relaxation effects in nuclear magnetic resonance absorption, Phys. Rev. 73 (1948) 679–712.
[28] J.T. Markert, E.J. Cotts, R.M. Cotts, Hydrogen diffusion in the metallic glass *a*-$Zr_3RhH_{3.5}$, Phys. Rev. B 37 (1988) 6446–6452.
[29] E.F.W. Seymour, Nuclear magnetic resonance studies of hydrogen diffusion in metal hydrides, J. Less Common. Met. 88 (1982) 323–334.
[30] G. Majer, G. Gottwald, U. Kaess, D.T. Peterson, R.G. Barnes, Nuclear relaxation in the deuterides of hafnium and titanium, Phys. Rev. B 68 (2003) 134304.
[31] A.V. Skripov, M. Pionke, O. Randl, R. Hempelmann, Quasielastic neutron scattering study of hydrogen motion in C14- and C15-type $ZrCr_2H_x$, J. Phys. Condens. Matter 11 (1999) 1489–1502.
[32] U. Eberle, G. Majer, A.V. Skripov, V.N. Kozhanov, NMR studies of hydrogen diffusion in the hydrogen-stabilized Laves-phase compound C15-$HfTi_2H_x$, J. Phys. Condens. Matter 14 (2002) 153–164.
[33] A.V. Skripov, Hydrogen diffusion in Laves-phase compounds, Defect Diffusion Forum 224–225 (2003) 75–92.
[34] M. Jansen, Volume effect or paddle-wheel mechanism – fast alkali-metal ionic conduction in solids with rotationally disordered complex anions, Angew. Chem. Int. Ed. 30 (1991) 1547–1558.
[35] M. Witschas, H. Eckert, H. Freiheit, A. Putnis, G. Korus, M. Jansen, Anion rotation and cation diffusion in low-temperature sodium orthophosphate: results from solid-state NMR, J. Phys. Chem. A 105 (2001) 6808–6816.
[36] H.-W. Meyer, F. Jurányi, D. Wilmer, Coupled anion and cation dynamics of silver orthophosphate in the picosecond range, Solid State Ionics 177 (2006) 3045–3049.